IJIRSET
International Journal of Innovative Research in Science | Engineering | Technology

ISSN(O): 2319-8753
ISSN(P): 2347-6710

International Journal of Innovative Research in Science Engineering and Technology (IJIRSET)

(A Monthly, Peer Reviewed, Refereed, Scholarly Indexed, Open Access Journal)

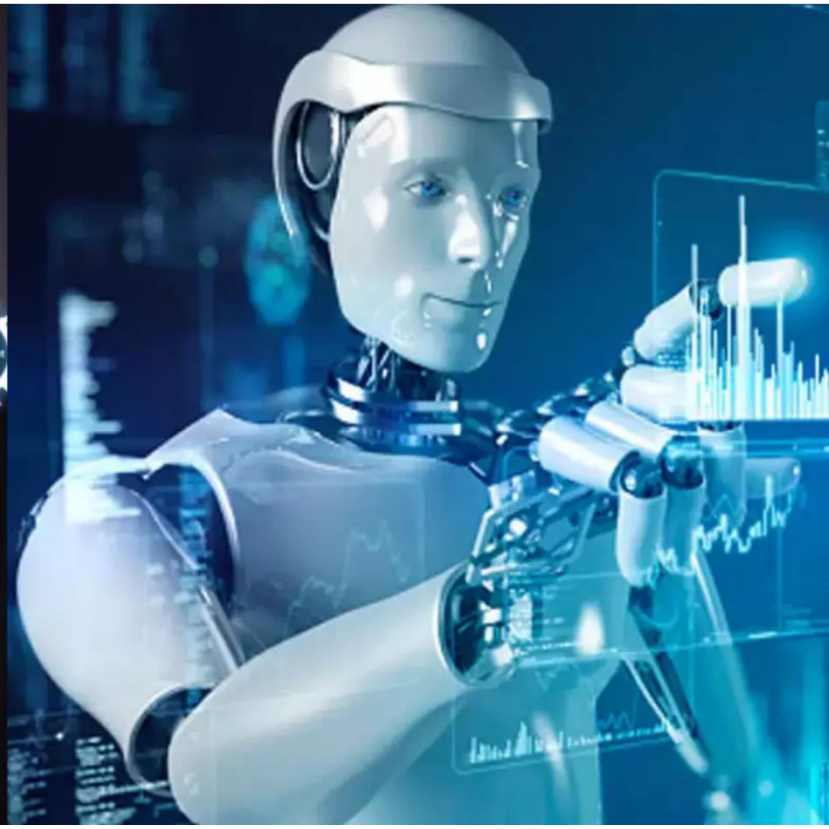

Impact Factor: 8.699

Volume 14, Issue 3, March 2025

International Journal of Innovative Research of Science, Engineering and Technology (IJIRSET)

Impact Factor 8.699

|www.ijirset.com |A Monthly, Peer Reviewed & Refereed Journal| e-ISSN: 2319-8753| p-ISSN: 2347-6710|

Volume 14, Issue 3, March 2025

|DOI: 10.15680/IJIRSET.2025.1403017|

Stability Analysis of Building Slopes with Foundation Weak Layers

FANG Weiqi, PENG Zhigao*, WU Di

College of Civil Engineering, Hunan City University, Yiyang, China

ABSTRACT: This study investigates the stability of building slopes containing foundation weak layers, with an emphasis on analyzing the mechanisms by which these layers influence cohesive strength reduction, pore pressure distribution, and critical thresholds of the slope safety factor (FOS). By developing a refined finite element model incorporating unsaturated soil behavior, the Mohr-Coulomb yield criterion, and cohesive reduction coefficients, the research elucidates the evolution of plastic strain and slip surface propagation within weak layers under seepage conditions. Key findings include: (1) Increased cohesive reduction accelerates slope destabilization due to material degradation, with weak layer strength reduction significantly lowering critical stability thresholds. (2) Plastic strain propagates along weak layers, deepening plastic zones and redirecting slip paths to deeper strata. (3) Nonlinear failure thresholds shift downward. These results provide critical theoretical insights and data support for slope engineering design, reinforcement strategies, groundwater management, and hazard monitoring systems in weak layer-prone regions.

KEYWORDS: slope stability; factor of safety; unsaturated soil; foundation weak layer; building slope

I. INTRODUCTION

With the acceleration of urbanization, building slopes serving as critical components of infrastructure engineering demonstrate vital significance in safeguarding human lives, property security, and regional economic development[1]. Recent years have witnessed extensive scholarly investigations into slope stability mechanisms. Duan[2] proposed a creep destabilization model for unsaturated loess slopes under extreme rainfall conditions, elucidating that the heterogeneous distribution of pore water pressure constitutes a pivotal trigger for potential slip surface formation. Through multiscale analysis, Li[3] revealed the susceptibility of loess-mudstone interfaces to shear zone development under moisture content fluctuations, a process that propagates progressive failure modes. Chen[4] corroborated via experimental-numerical hybrid approaches the spatiotemporal dominance of soil water content variations on plastic strain distribution patterns. These advancements have collectively established essential theoretical frameworks for slope stability assessment.

Nevertheless, practical engineering scenarios frequently encounter geological weak layers (e.g., fracture zones, low-permeability interlayers) formed through tectonic activities or weathering processes, which exhibit marked disparities in mechanical strength parameters (cohesion and internal friction angle) compared with adjacent soil masses[5]. Empirical studies indicate that such weak layers can accelerate slope failure through primary slip surface pathway propagation and hydraulic conductivity modification modalities[6]. For instance, Derbyshire et al. demonstrated that localized pore pressure anomalies induced by weak layers diminish shear strength by over 20%[7]. However, existing models predominantly rely on homogeneous assumptions, lacking systematic analysis of strength reduction effects associated with weak layers and their coupling mechanisms with critical safety factor (FOS) thresholds.

Addressing this scientific gap, this study develops a refined numerical model incorporating foundation weak layers through cohesion reduction coefficients, thereby unraveling their nonlinear destabilization mechanisms. The investigation bridges critical deficiencies in current theoretical frameworks while providing operational references for engineering risk mitigation.

International Journal of Innovative Research of Science, Engineering and Technology (IJIRSET)

Impact Factor 8.699

|www.ijirset.com |A Monthly, Peer Reviewed & Refereed Journal| e-ISSN: 2319-8753| p-ISSN: 2347-6710|

Volume 14, Issue 3, March 2025

|DOI: 10.15680/IJIRSET.2025.1403017|

II. FINITE ELEMENT MODELING OF BUILDING SLOPES AND PLASTICITY CRITERIA

The plastic potential of the building slope is described using the Mohr-Coulomb yield function [2]

$$F = m\sqrt{J_2} + \alpha I_1 - k \tag{1}$$

Among them, $\alpha = \frac{\sin\Phi}{3}, k = C\cos\Phi$

Parametric characterization of cohesion C and friction angle Φ is conducted as follows:

$$C = \frac{c}{FOS}, \Phi = \left(\frac{\tan\varphi_u}{FOS}\right)(P<0) + arc\tan\left(\frac{\tan\varphi_s}{FOS}\right)(P\geq 0) \tag{2}$$

where c represents the cohesion of the material, φ_u and φ_s denote the friction angles for unsaturated soil and saturated soil, respectively, and p indicates the pore pressure as given by Darcy's law.

This study employs COMSOL Multiphysics finite element analysis to address the aforementioned issues. A numerical model was established with a geometric weak layer thickness of 1.5 m. Other model dimensions, boundary conditions, and mesh configurations are illustrated in Figure 1, with computational parameters detailed in Table 1.

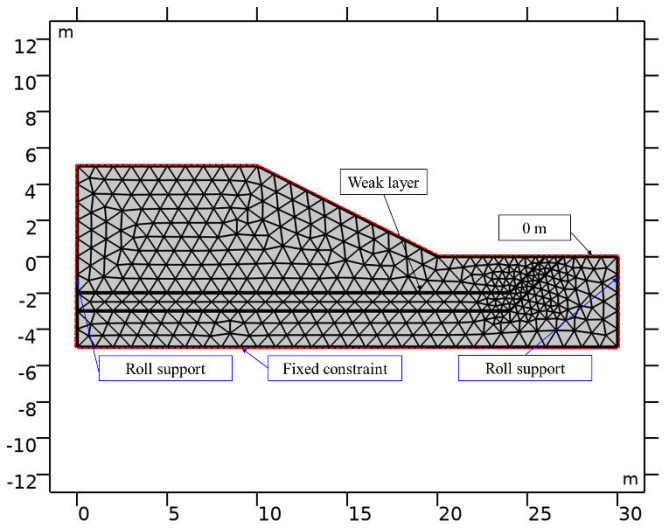

Figure 1 Illustrates the geometric dimensions of the model, boundary conditions, and meshing.

Table 1 Presents the detailed computational parameters.

Name	Symbolic	Value
Slope height /m	H	5
underground water level /m	H_w	4
Young's modulus /MPa	E	100
Poisson's ratio	μ	0.3
soil density /(kg/m^3)	ρ_{soil}	2000
water density /(kg/m^3)	ρ_w	1000
porosity	φ	0.3
cohesion /kPa	c	25
Friction angle of saturated soil /(°)	φ_{sat}	30

International Journal of Innovative Research of Science, Engineering and Technology (IJIRSET)

Impact Factor 8.699

|www.ijirset.com |A Monthly, Peer Reviewed & Refereed Journal| e-ISSN: 2319-8753| p-ISSN: 2347-6710|

Volume 14, Issue 3, March 2025

|DOI: 10.15680/IJIRSET.2025.1403017|

Friction angle of unsaturated soil /(°)	φ_{un}	20
Reduction coefficient of cohesion of weak layer	c_k/c	0.6~1.0

III. RESULTS AND DISCUSSION

Stability analyses across varying safety factors (FOS) revealed that numerical divergence occurred at FOS=2.5, signalling incipient slope instability. The pore pressure distribution Figure 2 displays pronounced heterogeneity along the vertical profile, spanning from -6.7 kPa to 83.3 kPa. Negative pore pressures predominantly concentrate within the upper 1.5 m of the slope crest, indicative of unsaturated conditions where matric suction enhances shear strength[1]^. Positive pressures extend from the phreatic surface (Hw=4 m) towards the slope toe, forming a hydraulic gradient of 30~60 kPa. This pattern demonstrates dynamic groundwater migration from high- to low-potential regions, reflecting both seepage dynamics and soil hydration states. Notably, negative pore pressures highlight unsaturated zones at the slope crest-critical features influencing global stability due to their shear strength variability.

Figure 3 demonstrates a 25-fold contrast in hydraulic conductivity between the unsaturated surface layer ($k=2\times10^{-5}$ m/s) and saturated zones ($k=5\times10^{-4}$ m/s). This disparity drives nonlinear decay of seepage velocities along the slope profile. Of particular engineering significance is the 60 kPa pore pressure observed near the slope toe, exceeding internal slope pressures by 12%, attributed to localized flow path convergence.

The identified slip surface (Figure 4) exhibits a composite circular-polygonal geometry. Progressive deformation manifests as shear-dominated displacement along the slope face, while tensile cracking dominates the crest region. Plastic zones (Figure 5) form a banded distribution along the slip surface, attaining maximum widths of 1.2 m. Peak strain values (7.58×10^{-4}) and displacements (1.11 mm) occur at the slope toe, escalating to 1.19 mm and 1.30 mm under progressive cohesion reductions of 0.8 and 0.6, respectively (Figure 6). These findings underscore the necessity of explicitly incorporating weak layer risks in slope design protocols.

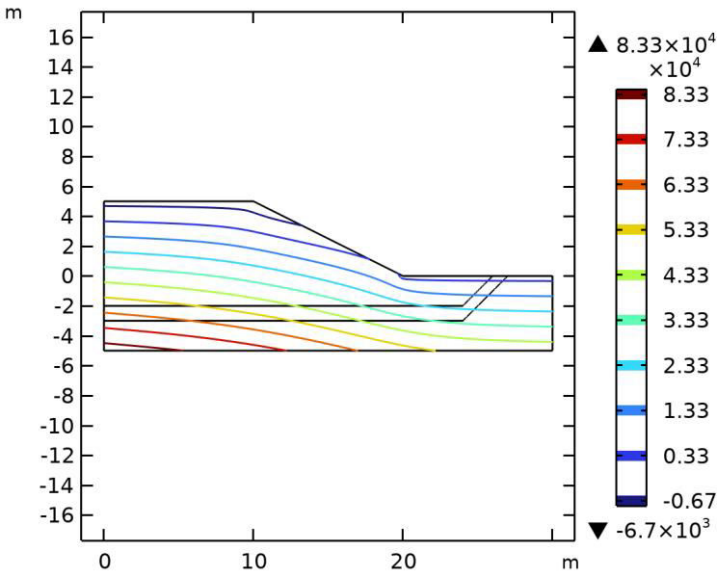

Figure 2 Pressure distribution (Pa)

International Journal of Innovative Research of Science, Engineering and Technology (IJIRSET)

Impact Factor 8.699

|www.ijirset.com |A Monthly, Peer Reviewed & Refereed Journal| e-ISSN: 2319-8753| p-ISSN: 2347-6710|

Volume 14, Issue 3, March 2025

|DOI: 10.15680/IJIRSET.2025.1403017|

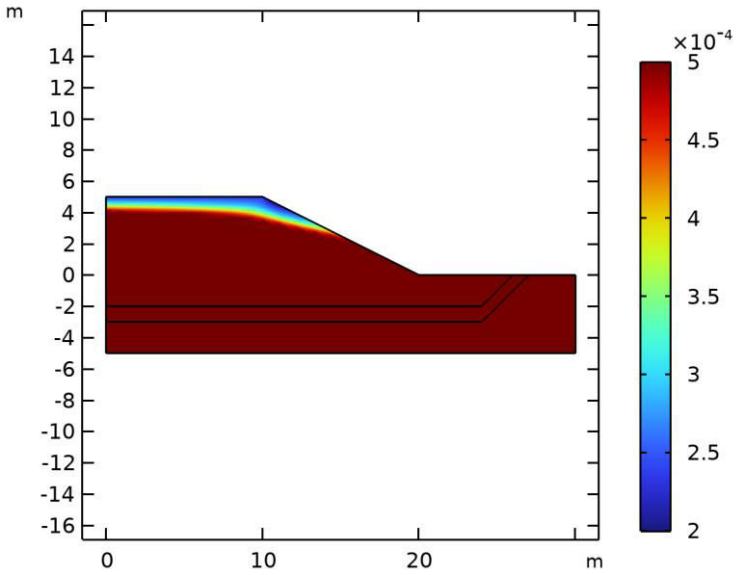

Figure 3 Hydraulic conductivity (m/s)

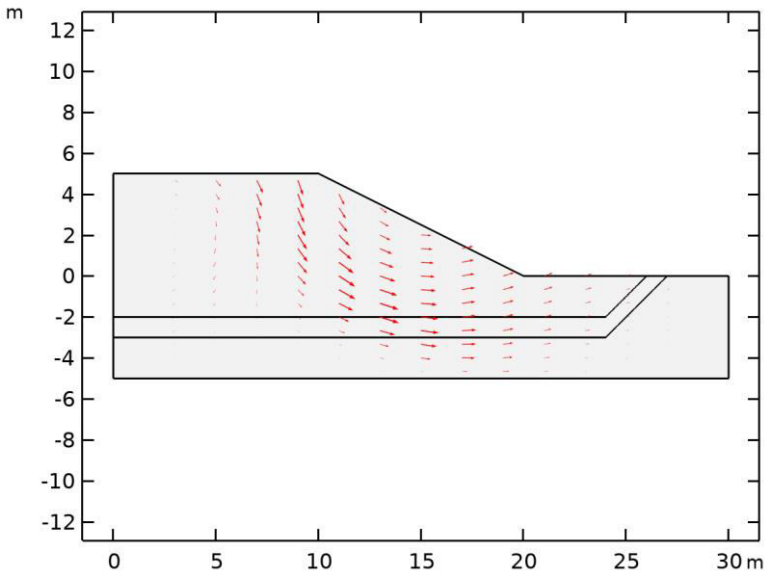

Figure 4 Slip surface

International Journal of Innovative Research of Science, Engineering and Technology (IJIRSET)

Impact Factor 8.699

|www.ijirset.com |A Monthly, Peer Reviewed & Refereed Journal| e-ISSN: 2319-8753| p-ISSN: 2347-6710|

Volume 14, Issue 3, March 2025

|DOI: 10.15680/IJIRSET.2025.1403017|

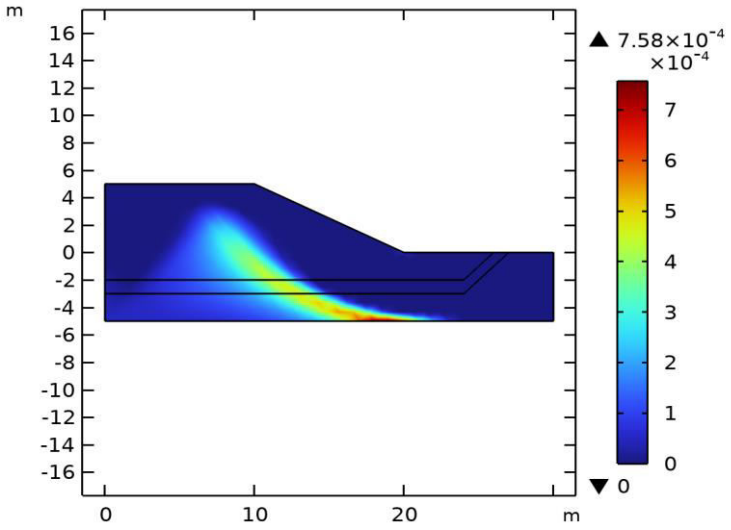

Figure 5 Equivalent plastic strain

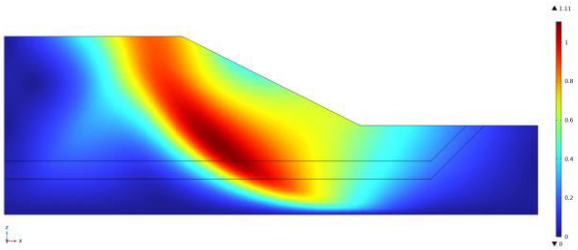

(a) $c_{weak}/c=1.0$

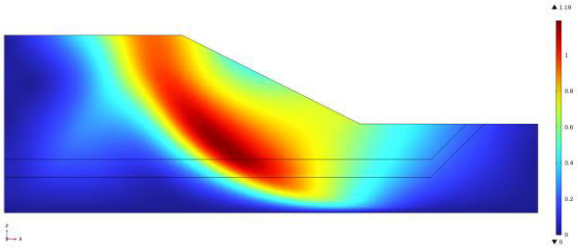

(b) $c_{weak}/c=0.8$

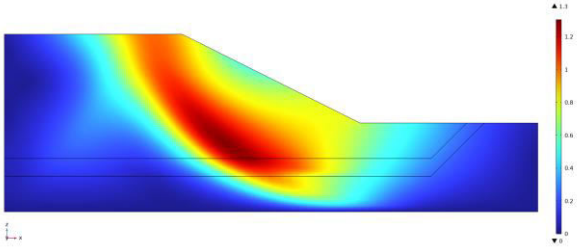

(c) $c_{weak}/c=0.6$

Figure 6 Displacement (mm)

International Journal of Innovative Research of Science, Engineering and Technology (IJIRSET)

Impact Factor 8.699

|www.ijirset.com |A Monthly, Peer Reviewed & Refereed Journal| e-ISSN: 2319-8753| p-ISSN: 2347-6710|

Volume 14, Issue 3, March 2025

|DOI: 10.15680/IJIRSET.2025.1403017|

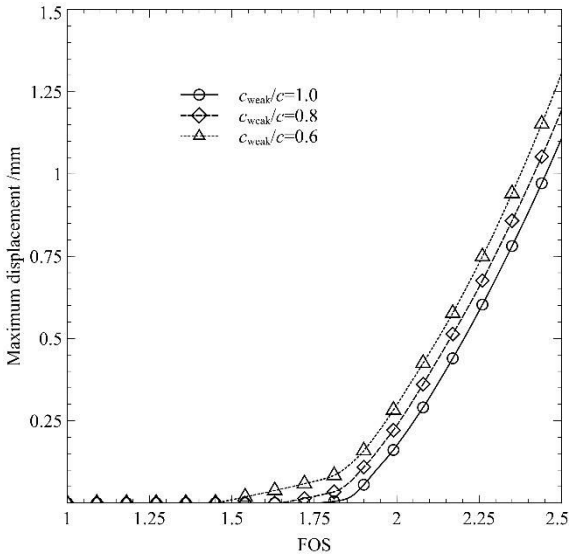

Figure 7 Relationship between maximum displacement and safety factor FOS

Figure 7 illustrates the variations in maximum slope displacement with safety factor (FOS) under different cohesion reduction coefficients. The results demonstrate a nonlinear escalation of maximum displacement as FOS increases. When FOS < 1.4, displacement growth exhibits negligible rates, remaining below detectable thresholds. Across the transitional FOS range of approximately 1.4~1.8, maximum displacements gradually rise to 0.1 mm, signaling incipient mechanical degradation. A critical inflection occurs at FOS > 1.8, where displacements surge rapidly, with escalation magnitudes inversely correlated to cohesion reduction coefficients (i.e., lower coefficients induce greater displacement increments). This nonlinearity implies that slope deformation is not merely linearly proportional to FOS but transitions abruptly beyond a critical FOS threshold, triggering accelerated destabilization. Significantly, the presence of weak layers amplifies this instability mechanism by exacerbating displacement accumulation, particularly under reduced cohesion conditions. The observed trends underscore the necessity of identifying critical FOS thresholds and quantifying weak layer effects in stability assessments to mitigate abrupt failure risks.

IV. CONCLUSION

This study systematically investigates the nonlinear destabilization mechanisms induced by cohesion degradation in foundation weak layers within unsaturated building slopes through refined finite element modeling, yielding the following principal conclusions:

(1) Hydraulic-Geomechanical Coupling in Weak Layers: Foundation weak layers exacerbate slope instability by modifying seepage fields and plastic strain distributions. Numerical simulations reveal that the 1.5 m unsaturated soil layer at the slope crest generates a negative pore pressure zone (-6.7 kPa), which enhances matric suction. Concurrently, a high-pore-water-pressure region (83.3 kPa) at the slope toe establishes a hydraulic gradient across the weak layer. This gradient induces a 25-fold contrast in hydraulic conductivity (2×10^{-5} m/s vs. 5×10^{-4} m/s), concentrating seepage pathways within the weak layer.

(2) Cohesion-Dependent Failure Modes: Cohesion reduction coefficients critically govern slope failure mechanisms. Reducing the coefficient from 1.0 to 0.6 elevates maximum displacement by 17%, accompanied by a lateral expansion of the plastic strain band to 1.2 m.

(3) Nonlinear Stability Evolution: Displacement growth transitions to accelerated instability when the safety factor (FOS) exceeds 1.8, particularly under cohesion reduction coefficients ≤0.6. Beyond this threshold, sustained creep deformation develops, with slip surfaces preferentially propagating along weak layers to form continuous failure channels.

International Journal of Innovative Research of Science, Engineering and Technology (IJIRSET)

Impact Factor 8.699

|www.ijirset.com |A Monthly, Peer Reviewed & Refereed Journal| e-ISSN: 2319-8753| p-ISSN: 2347-6710|

Volume 14, Issue 3, March 2025

|DOI: 10.15680/IJIRSET.2025.1403017|

These findings elucidate slope destabilization mechanisms governed by unsaturated soil-weak layer interactions, providing a theoretical foundation for safety assessments of slopes in analogous geological settings. The study emphasizes the necessity of integrating weak layer dynamics into probabilistic stability analyses to mitigate sudden failure risks in engineering practice.

REFERENCES

[1]ORTIZ-ZAMORA D, ORTEGA-GUERRERO A. Evolution of long-term land subsidence near Mexico City: Review, field investigations, and predictive simulations: LONG-TERM LAND SUBSIDENCE[J/OL]. Water Resources Research, 2010, 46(1)[2023-04-19].
[2]DUAN G, SONG F, WANG H, et al. Stability analysis of unsaturated loess slopes subjected to extreme rainfall incorporating creep effects[J]. Computers and Geotechnics, 2024, 169: 106231.
[3]Li L, Datcheva M, Baille W. Coupled thermo-hydro-mechanical finite element simulation of loess slope under atmospheric boundary conditions[M]//Georgiev I, Kostadinov H, Lilkova E. Advanced Computing in Industrial Mathematics: Vol. 961. Cham: Springer International Publishing, 2021: 244-255.
[4]Chen L, Peng J, Xie F, et al. Effect of moisture content on the time-dependent mechanical characteristics of loess[J]. Environmental Earth Sciences, 2022, 81(7): 217.
[5]Turkson P, VandenBerge D R. Rapid drawdown analysis of levees[J]. Journal of Geotechnical and Geoenvironmental Engineering, 2025, 151(1): 4024154.
[6]Li S, Li C, Yao D, et al. Multiscale nonlinear analysis of failure mechanism of loess-mudstone landslide[J]. Catena, 2022, 213: 106188.
[7]Derbyshire E, Dijkstra T A, Smalley I J, et al. Failure mechanisms in loess and the effects of moisture content changes on remoulded strength[J]. Quaternary International, 1994, 24: 5-15.

Funding: This research was supported by Undergraduate Innovation and Entrepreneurship Training Program of Hunan Province (Grant No. S202311527023); Yiyang City Science and Technology Innovation Plan Project (Yiyang Financial and Education Measures [2023]102); Hunan Provincial Natural Science Foundation of China (Grant No. 2023JJ50345).

INTERNATIONAL STANDARD SERIAL NUMBER INDIA

INNO SPACE SJIF Scientific Journal Impact Factor

doi cross ref

निस्केयर NISCAIR

INTERNATIONAL JOURNAL OF INNOVATIVE RESEARCH

IN SCIENCE | ENGINEERING | TECHNOLOGY

9940 572 462 6381 907 438 ijirset@gmail.com

www.ijirset.com

Scan to save the contact details